Article citation info:
Giechaskiel B, Melas A, Mamakos A. Assessment of two condensation particle counters (CPCs) in photometric mode for high concentration exhaust emission measurements. Combustion Engines. 2023;193(2):15-23. https://doi.org/10.19206/CE-161190

Barouch GIECHASKIEL
Anastasios MELAS
Athanasios MAMAKOS

Combustion Engines
Polish Scientific Society of Combustion Engines

Assessment of two condensation particle counters (CPCs) in photometric mode for high concentration exhaust emission measurements

ARTICLE INFO

Received: 31 December 2022
Revised: 12 February 2023
Accepted: 13 February 2023
Available online: 14 February 2023

Condensation particle counters (CPCs) use light scattering to count particles after they have grown to micron size in a supersaturated environment. In single counting mode each particle is counted depending on whether the scattered light exceeds a threshold value or not. In photometric mode the total scattered light is converted in particle number concentration. While for laboratory grade particle number systems, CPCs are allowed to operate only in single counting mode, there is no such requirements for portable emissions measurements systems (PEMS) for real-driving emissions (RDE) testing or for instruments for periodic technical inspection (PTI) of vehicles. In this study two CPCs of the same model were assessed in single counting and photometric modes with silver and graphite particles with sizes ranging from 10 nm to 100 nm. The results showed that the concentration was measured accurately enough for particles in the 25 nm to 50 nm size range, but was underestimated and overestimated for smaller and larger particles, respectively. The key message is that the photometric mode should be avoided or calibrated in function of concentration and particle size.

Key words: *PEMS, PTI, CPC, PNC, single counting mode, photometric mode*

1. Introduction

The particulate matter (PM) emissions from diesel vehicles are regulated since the beginning of the 1990s in the United States of America (USA), European Union (EU) and Japan. Other countries, such as China and India, introduced limits at the beginning of 2000. The method is based on (i) testing the vehicle over a prescribed test cycle on a chassis dynamometer; (ii) weighing of a filter that collected PM from a diluted part of the exhaust gas. The introduction of particulate filters at the exhaust aftertreatment of diesel vehicles rendered the filter method unsuitable due to the low mass of the collected PM. Furthermore, concerns that ultrafine particles might have more adverse health effects than bigger particles for the same mass led to assessment of a particle counting method for regulatory purposes. This was tasked in 2003 to the particle measurement programme (PMP) informal group of the United Nations Economic Commission for Europe (UNECE). Dedicated evaluations and inter-laboratory studies confirmed the suitability of the particle number (PN) counting method for introduction in the regulations [1]. The PN method was introduced in the EU regulation for light-duty diesel vehicles in 2011. The PM and PN limits were extended to gasoline vehicles with direct injection engines, heavy-duty engines, and non-road mobile machinery (NRMM) [2, 3]. A similar method has also been proposed for measurement of particles from brake emissions [4].

A further big step in the EU regulation was the control of vehicles on the road with portable emissions measurement systems (PEMS) during real-driving emissions (RDE) testing [5–8]. On-board vehicle testing requires small, lightweight instruments and consequently the technical requirements of the laboratory grade equipment were relaxed for PEMS. Laboratory grade systems require calibration of the thermal pre-treatment unit and the particle number counter (PNC) separately. On the other hand, PEMS can be calibrated as a complete unit. Most importantly, while the laboratory grade systems have condensation particle counters (CPCs) for counting the particles, PEMS can have any detector, as long as they fulfil the counting efficiency requirements. CPCs are instruments that optically count particles using light scattering after their growth to micron size in a supersaturated environment [9, 10]. The CPCs of the laboratory systems have strict linearity requirements (±5%), while the PEMS more relaxed (±15%) [2].

The previous discussion was referring to instrumentation for the type-approval and in-service conformity (ISC) of the vehicles, which is responsibility of the vehicle manufacturers. The same instrument requirements apply for the market surveillance, which is responsibility of type-approval authorities and the European Commission. Type-approval, ISC or market surveillance is conducted on a limited number of vehicles from the vehicle fleet. On the other hand, every vehicle circulating in the market needs to be tested for its roadworthiness every few years. This is responsibility of the vehicle owner, who brings the vehicle to an appropriate testing center for the periodic technical inspection (PTI). The control of the PM is conducted with an opacity meter only for diesel vehicles. The opacity measurement however, is not appropriate for particulate filters equipped vehicles, because it can hardly detect a removed or tampered particulate filter [11, 12]. A new PN methodology was introduced in Belgium in July 2022, while the Netherlands, Germany and Switzerland will introduce the new methodology in 2023. The sensors that are used are handheld devices designed for garage environment. Thus, their technical specifications are even more simplified than for PEMS. There is no requirement for the principle of operation of the detector, and the linearity accuracy requirements are ±25%.

Laboratory grade CPCs have to be used in single counting mode, while for PEMS or PTI devices there is no such

requirement, and thus, the use of the photometric mode is not excluded. In single counting mode the particle concentration is determined by counting discrete events of light scattered by a particle(s) passing through an inspection volume. The light scattered creates an electric pulse, which above a threshold value is considered a particle count. Internal corrections such as for coincidence for older CPCs, or dead/live time for newer CPCs are typically applied. In photometric mode the concentration is determined by a bulk measurement of the amount of light scattered by a particle(s) passing through the inspection volume. Corrections include functions that turn the photometric measurement into a concentration. In theory, the photometric mode could be used for single particles counting as well. However, the accuracy is not as good as with single counting mode because of the sixth power dependence of light scattering intensity on particle size for particles small compared to the wavelength of scattered light [9, 10]. Thus, the transition between the two modes is typically done at some upper limit, typically when the internal single counting mode corrections reach a 10–20% value. The transition concentration is between 10^4 #/cm^3 to 10^5 #/cm^3, depending on the CPC model. The PTI limit in Belgium and the Netherlands is 10^6 #/cm^3, thus a CPC with a 10:1 dilution, in principle, could avoid the use of the photometric mode. The tailpipe exhaust concentrations measured by PEMS can be as high as 10^8 #/cm^3 [13]. A dilution of 1000:1 could avoid the use of the photometric mode, but for typical dilutions of 100:1 there will be instances that the CPC measures in the photometric mode.

In theory, once calibrated, the photometric mode should remain in acceptable levels of accuracy (±20%) independently of the original type of particles, because all particles grow in similar sizes in the micrometer range before detection and they should have the same refractive index due to the condensed vapor of the working fluid. However, recently we found that small silver particles were underestimated at least 40% compared to soot particles [14]. There are not many studies that have examined the photometric mode range of CPCs, and even less any size dependency [15]. The knowledge on the topic is based on studies on the growth of particles in the CPCs at low particle number concentrations [9, 16], but has not been expanded to high concentrations. Furthermore, usually, CPCs are not accompanied with calibration certificates for the photometric range and thus the true uncertainty at these high levels is not well known. Current regulations for PEMS and PTI devices permit the photometric mode and different materials can be used for calibration. For example, for PEMS only soot-like particles are permitted, while for PTI additionally salt or other materials can be used. Furthermore, for PEMS calibration is done at sizes > 45 nm, while for PTI between 70 and 80 nm. Consequently, the main questions raised are (i) what is the uncertainty of the photometric mode and (ii) whether the uncertainty can be kept at low levels with specific calibration requirements. In order to address these questions, and cover this gap in the literature, in this study we compare two identical CPCs in both single and photometric counting modes with different materials (graphite, silver) and different sizes. The results of this study are not useful only for vehicle exhaust emission measurements [17–19], but any other aerosol measurement field (e.g. nanomaterials, ambient air, work exposure) [20, 21].

2. Materials and methods

Figure 1 presents the experimental setup. Two particle generators were used to generate particles of different materials (graphite or silver) and sizes: the geometric mean diameter (GMD) ranged from below 10 nm up to 100 nm. Silver particles are typically small (< 20 nm) and can be assumed that they resemble more the metal oxides from the lubricant. Graphite particles have similarities with soot particles from combustion engines [22, 23]. Furthermore, vehicle exhaust regulations require the measurement of the non-volatile (solid) particles, thus the silver and graphite particles of this study should be representative of the results expected with exhaust particles.

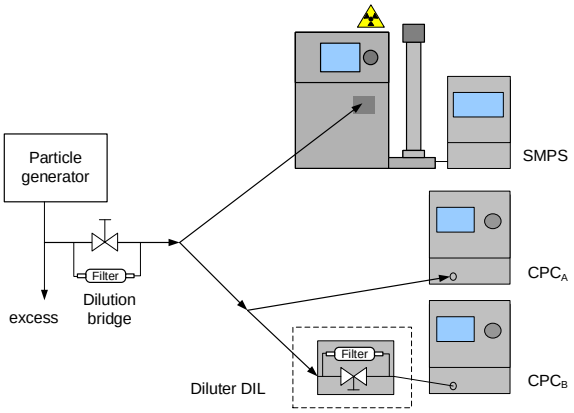

Fig. 1. Experimental setup. With dotted lines we indicate instruments that were optionally used

The concentration was further decreased in a dilution bridge. The size distributions were determined by a scanning mobility particle sizer (SMPS) with a long differential mobility analyzer (DMA) 3081, and a 3010 butanol CPC with 50% efficiency at 10 nm (SMPS model 3936, TSI Inc., Shoreview, MN, USA). Corrections for multiply charged particles and diffusion losses were applied by the manufacturer's aerosol instruments manager (AIM) software version 9.0.0. The SMPS was evaluated before the measurement campaign [14]. In parallel to the SMPS, two identical CPCs were measuring; one of them optionally with a diluter (DIL). The protocol included tests at different concentration levels adjusting the dilution bridge. The SMPS due to its lower resolution time (around 2.5 min) was not used at all concentrations steps, but at indicative intervals. For silver particles only part of the size distribution was captured by the SMPS. The missing part was taken into account by fitting the measured part (Fig. 2). The "missing" part below 7.5 nm was around 28–30%, while below 4 nm around 0.5–1.5%. The correction of the particle concentration for the "missing" part was between 1.35 and 1.55. Details for the instruments follow.

2.1. Particle generators

The DNP 3000 (Palas GmbH, Karlsruhe, Germany) produces graphite particles by high-voltage spark discharges between two graphite electrodes in a N_2 flow [24]. Sub-

sequent internal dilution with filtered air reduces the particle number concentration. The two settings used were: (i) for GMDs 25 nm to 50 nm: medium energy 3.0 kV, current 2 mA, N_2 carrier 3 dm^3/min, mixing air 8 dm^3/min; (ii) for GMDs 60 nm to 100 nm, medium energy 3.0 kV, current 5 mA, N_2 carrier 3 dm^3/min, mixing air 3 dm^3/min. The size was adjusted by modifying the residence time in the tubing between the generator and the instruments.

Silver particles were generated by an in-house tungsten glowing wire generator (GWG) [25]. Accordingly, a silver filament was placed around tungsten. The silver filament was heated resulting in silver vapors. N_2 was used as carrier gas to avoid oxidation of the tungsten wire and the silver particles. The carrier gas was further mixed with N_2 to reduce the silver particles concentration.

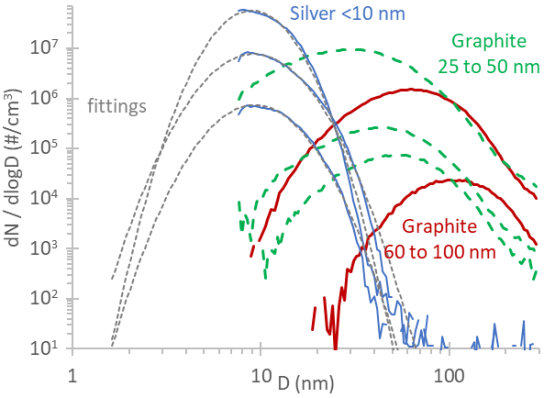

Fig. 2. Examples of particle number size distributions measured by SMPS. Grey dotted lines present the fittings to the measured silver size distributions

2.2. Condensation Particle Counters (CPCs) model 3752

Two identical butanol CPCs (model 3752, TSI) with 50% efficiency at 4 nm were measuring the particle number concentration [26, 27]. The CPCs were used with 1.5 dm^3/min flowrate. From this flow, 0.3 dm^3/min pass through the optics, while the 1.2 dm^3/min bypass the optics. Flow rate measurements confirmed that these flows were within 5% of the nominal values. One of them (CPC_A) was calibrated 10 months before the measurement campaign. The other (CPC_B) was calibrated three years before the measurement campaign. However, due to the COVID-19 lockdown, its use the last two years was limited. All calibration certificates, for the initial and subsequent calibrations, included only a single check in single counting mode at 50,000 #/cm^3, and no information on the photometric mode. This certificate calibration factor was taken into account in the results.

2.3. Diluter (DIL)

One of the CPCs (CPC_B) was also used downstream of a diluter (model DDS 560, Topas GmbH, Dresden, Germany) in order to keep the concentrations in the single counting mode. The principle was similar to the dilution bridge concept (i.e. bifurcated diluter). A fixed dilution of 50:1 was used for all tests. We calibrated the diluter (DIL) at this specific dilution 50:1 before the measurement campaign. The penetration with silver and graphite particles is given in Fig. 3. The procedure was according to the regulation for particle number systems: Regulation (EU) 2017/1151. The penetration was around 95% for 25 nm particles, 82% for 15 nm, 60% for 8 nm. Based on the fitting of the experimental data and to take into account the particle losses: a 1.05 correction was applied when 25 nm size distributions were measured with graphite particles and 1.65 for 8 nm size distributions with silver particles.

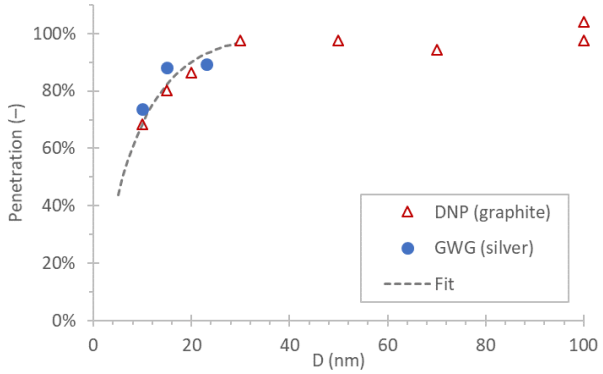

Fig. 3. Penetration of diluter DIL with silver and graphite particles at dilution ratio 50:1

3. Results

3.1. Inter-comparison of CPCs

Figure 4 plots the difference of the two CPCs at various concentrations. The tests were conducted without any dilution upstream of the CPCs, thus the "raw" concentrations refer to the readings of the CPC (including the certificate calibration factors).

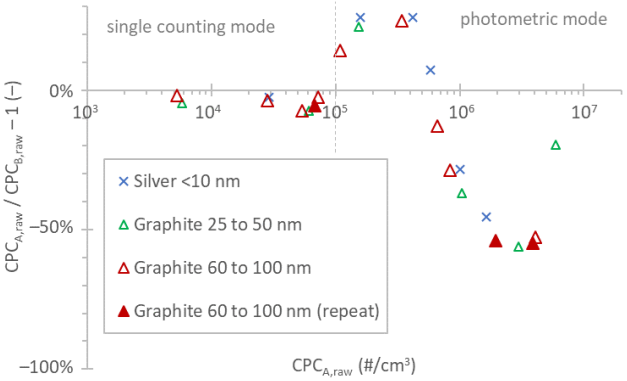

Fig. 4. Comparison of CPC_A with CPC_B. No dilution DIL was used upstream of any CPC. CPC_{raw} refers to the concentration measured by the CPC, including the certificate calibration factors

Up to 10^5 #/cm^3, the differences were within 5%. Then the differences followed a wavy curve: they increased up to 25% at concentrations 2–4×10^5 #/cm^3, then they decreased to –55% at concentrations 2–4×10^6 #/cm^3, and then they further increased. The behavior was independent of the material or the size distribution. Since these are nominally the same devices, this behavior points towards inaccurate calibration at high concentrations. The actual correction applied in photometric mode is not known. From this comparison it was not clear which CPC was the correct one, if any of the two. It should be noted that the calibration certificates of the specific CPCs included only one point in the

single counting mode at 5×10^4 #/cm^3, and no points in the photometric mode.

3.2. CPC vs. SMPS

Figure 5 and Figure 6 compare CPC_B and CPC_A, respectively, with SMPS for various materials and size distributions. The SMPS silver particle size distributions were corrected by a factor 1.35 to 1.55 depending on the missing part of the size distributions (see Fig. 2). The y-axis plots the difference of the corrected CPC concentration (i.e. certificate calibration factor, dilution ratio, diluter losses) to the SMPS. The x-axis plots the raw CPC concentration, i.e. without dilution correction (if any).

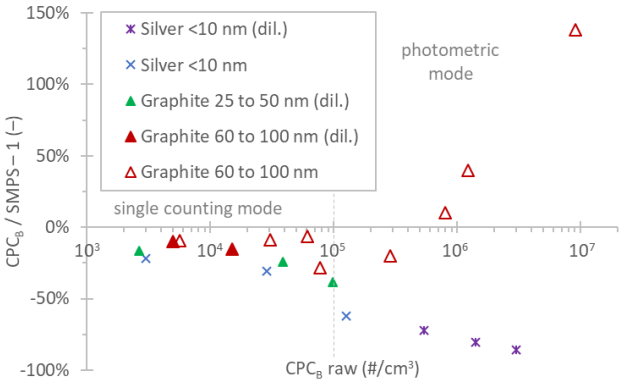

Fig. 5. Comparison of CPC_B with SMPS. "dil." indicates measurements that the CPC_B was used downstream of the diluter

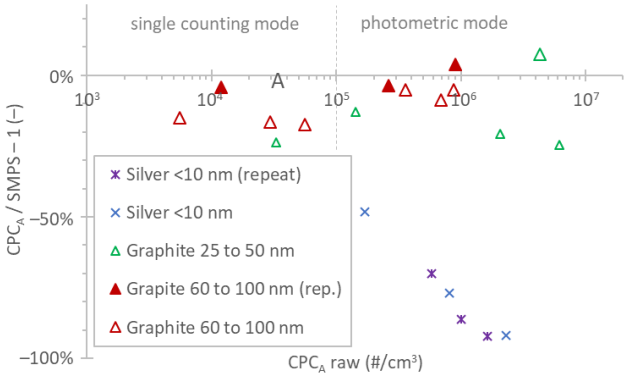

Fig. 6. Comparison of CPC_A with SMPS

The measurements with graphite particles resulted in a reasonable agreement with the SMPS (5% to 40%) [28] for both CPCs up to a concentration of 10^5 #/cm^3 and up to the maximum concentration of 10^7 #/cm^3 for CPC_A. In the photometric mode, the two CPCs showed different trends partly in agreement with their relative comparisons, as presented in Fig. 4.

The comparison to the SMPS, however, revealed a consistent effect of the aerosol in the CPC/SMPS correlations. In particular, both CPCs were found to measure systematically lower concentrations of silver particles, with the difference increasing with the concentration reaching as high as –90% at 10^7 #/cm^3 (i.e. one order or magnitude lower).

3.3. CPC_A vs. CPC_B downstream of a diluter

The uncertainties associated with the SMPS data inversion including the external correction for the undetected fraction of the silver particle distribution, can raise concerns. Furthermore, high concentrations of charged particles, if not properly neutralized, can lead to overestimation of the SMPS concentrations. For example, the graphite particles can be highly charged [29] or high charges from the glowing wire generators have been reported [30]. In order to confirm that the findings were true and not experimental errors we repeated some tests using CPC_B downstream of the diluter as reference instrument. The CPC concentrations, when used in single counting mode, should be very accurate, but CPCs, do not give size information. Figure 7 compares the readings of CPC_A without any dilution to the readings of CPC_B corrected with the dilution 50:1 of the upstream diluter. Thus, the concentrations measured by CPC_B were approximately 50 times lower than those shown in the x-axis of Fig. 7 and always in single counting mode. Furthermore, particle losses for the diluter according to Fig. 3 were applied.

For concentration levels up to 10^5 #/cm^3 the differences were within ±5% for graphite or ±10% for silver particles. When the two CPCs were compared to each other, their differences were within ±5% (Fig. 4). The higher variability with silver particles (10% vs. 5%) had to do with the uncertainty of the particle loss corrections for the diluter DIL. Nevertheless, the variability is smaller than when the CPCs were compared to the SMPS (Fig. 4 and 6).

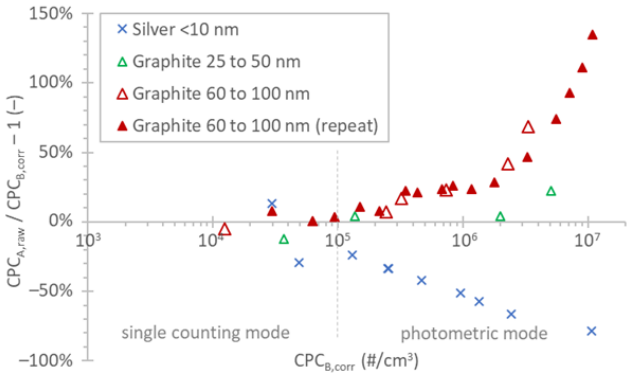

Fig. 7. Comparison of CPC_A with CPC_B downstream of diluter DIL; $CPC_{B,corr}$ refers to the concentration after correction with the dilution ratio of DIL 50:1, certificate calibration factors, and losses in the diluter DIL; $CPC_{B,raw}$ was always in the single particle mode

In the photometric mode, CPC_A underestimated the concentrations for silver particles. On the other hand, it overestimated the concentration for large graphite particles at concentrations > 10^6 #/cm^3. Only for the 25 to 50 nm graphite particles the differences remained within 20%.

The results were very similar to those of Fig. 6, where the reference was a SMPS, confirming the reliability of the data. The results and trends were also very similar with those of CPC_B (Fig. 5). However, as noted also in Fig. 4, for concentrations > 1×10^6 #/cm^3 CPC_A was measuring much lower, or as the previous results showed, CPC_B was actually measuring much higher (overestimating). Combining the information from Fig. 5–7 it can be concluded that the calibration of CPC_A in the photometric mode was more accurate.

4. Discussion

This study addressed a critical question: what is the uncertainty of the photometric mode of the CPCs. While CPCs for laboratory grade equipment are allowed to operate only in the single counting mode, there is no such requirement for PEMS and PTI. Thus, it was important to evaluate whether the uncertainty remains within 15% for PEMS and 25% for PTI instruments, as prescribed in the relative regulations. It should be emphasized that the specific CPCs that we evaluated are not used for PEMS or PTI testing, and the aim of this study was to assess the principle of photometric mode in such applications, and not the specific CPCs per se.

The results showed that in most cases, a calibrated CPC, can remain within 25% (Fig. 6), which includes also the uncertainty of the reference system. This value is close to the one typically reported as uncertainty for photometric mode (20%) from the instrument manufacturer. The results were confirmed using either a SMPS as reference instrument or a CPC downstream of a diluter measuring in single counting mode. However, the results also revealed that: (i) for very small particles (around 10 nm) the concentration was underestimated; (ii) for very large particles (> 60 nm) the concentration can be overestimated; (iii) the deviations depended on the concentration levels; (iv) the two CPCs had large differences in the photometric mode.

This is one of the few studies that have examined the high concentration (photometric) range of the CPCs, and probably the first one that covered from very small to large particle sizes (range at least 10 nm to 100 nm). It is also the first study that raises concerns for the photometric mode for large sizes. The assessment of the photometric mode (principle) at low concentrations is not something new. The first photoelectric instrument was developed early in 1940 [9]. The aerosol was saturated by diffusion of water vapor. The subsequent expansion to atmospheric pressure produced cloud by condensation. The attenuation was measured with a photoelectric cell. Such an instrument developed in 1970s was capable of reaching concentrations up to 10^6 #/cm^3 [31]. A commercially available and commonly used instrument since the 1980s was the TSI model 3020 [32]. It operated in the photometric mode for concentrations higher than 1000 #/cm^3. The photometric mode was based on the scattered light by the aerosol cloud and an empirical calibration. The successor was the TSI model 3022A using butanol as a working fluid, which was replaced by model 3775 and later by 3752, the model that was assessed in our study.

The first question would be how the photometric mode is calibrated and which are the reported deviations reported in the literature. Calibration of the first photoelectric counters was conducted with a "tube bridge" or dilution bridge in mid-1940s and polydisperse aerosol, which practically halved the aerosol concentration [33]. Since the 1970s the preferred method was, and still is, using monodisperse aerosol with a differential mobility analyzer (DMA) and determination of the concentration with an electrometer [9]. Our tests were a combination of the two methods: We used a DMA and a diluter upstream of the reference CPC. By characterizing the diluter, it was possible to minimize the measurement uncertainty.

One study [34] with a CPC model 3022 found a constant deviation of 20–30% for concentrations up to 4×10^5 #/cm^3 for polydisperse 35 nm and 92 nm NaCl, 82 nm carbon, 111 nm and 233 nm di-ethyl-hexyl-sebacate (DEHS) particles. However, higher concentrations were not tested. Others have tested the transition from single counting mode to photometric mode and noticed differences for a Grimm 5.401 CPC [35], a TSI 3022A [36] and a water CPC [37]. The only study with high concentrations, up to 10^7 #/cm^3 [15], compared many instruments with various polydisperse materials. The 3022A was within 5% of the average value for concentrations up to 10^5 #/cm^3 for all materials. At higher concentrations the deviation was much higher: -65% at 2×10^6 for 7 nm silver, –30% at 5×10^5 for 11 nm tungsten oxide, –50% at 5×10^5 for 20 nm NaCl, but +20% at 5×10^6 for 130 nm DEHS particles. However only two instruments could measure above 10^6 #/cm^3. The findings demonstrate large deviations in the photometric mode, that depend on the particle size. Thus, our results are in good agreement with the literature.

Even though there is only one study that examined the photometric mode experimentally and there was no "true" reference, insight for the measured deviations can be gained by older studies at low concentration levels. Already in the early 1980s researchers observed that pulse heights produced by the photodetector of the TSI 3020 decreased with decreasing particle size for particles smaller than 15–20 nm [9]. The super-saturation that is required to activate condensational growth increases as droplet sizes decrease (Kelvin effect). Saturation ratios increase from a value of unity near the condenser inlet to a maximum in the midsection [38–41]. Due to the Kelvin effect, smaller particles travel further in the condenser before their activation and therefore they have less time to grow, resulting in lower scattered light and pulse height. For example, when the flow rate of a TSI 3020 decreased from 300 to 200 cm^3/min, the counting efficiency of 5 nm particles increased by as much as six-fold, indicating that the particles grew more in size [42]. However, too low flowrate can result in excessive particle losses before their growth. Particles activated near the entrance of the condenser reach similar final sizes and produce similar pulse heights [43].

Extrapolating the findings of the above mentioned studies from low to high particle concentrations, it can be derived that the signal of the photometric mode depends on the initial particle size when at the steep part of the counting efficiency curve. Figure 8a plots the ratio of the CPC_A to the SMPS in function of the GMD of the measured size distributions. The data are based on Fig. 6 with a correction factor of 1.15 to bring the ratio to 100% at large sizes. The reason of this 15% correction was not investigated in detail, but is well within expected differences between SMPS and CPCs [44, 45]. The same figure plots (dotted line) the expected ratio measuring polydisperse aerosol, based on the monodisperse counting efficiencies found in the literature for the specific CPC model [27]. Small symbols are measurements in photometric mode, while big symbols in single counting mode. Figure 8b plots the same information for

CPC_B. Although the single counting mode (large) points lay on the expected curve, the measurements in photometric mode of small particles are much lower. In single counting mode the pulse height is not important because each particle is counted, as long as the pulse height is above a threshold level. In photometric mode, the total scattered light is translated into particle concentration. Since the scattered light from each particle is lower for small particles, the total scattered light and the resulting concentration will be lower.

The pulse height depends on the final particle size and consequently on the saturation profile. The saturation profile depends on the geometry and the operating conditions of the CPC, which determine the heat and mass transfer [43]. Thus, different CPC models with differences in saturator temperatures will have different super-saturation ratios (and profiles) and thus different droplet growth [38].

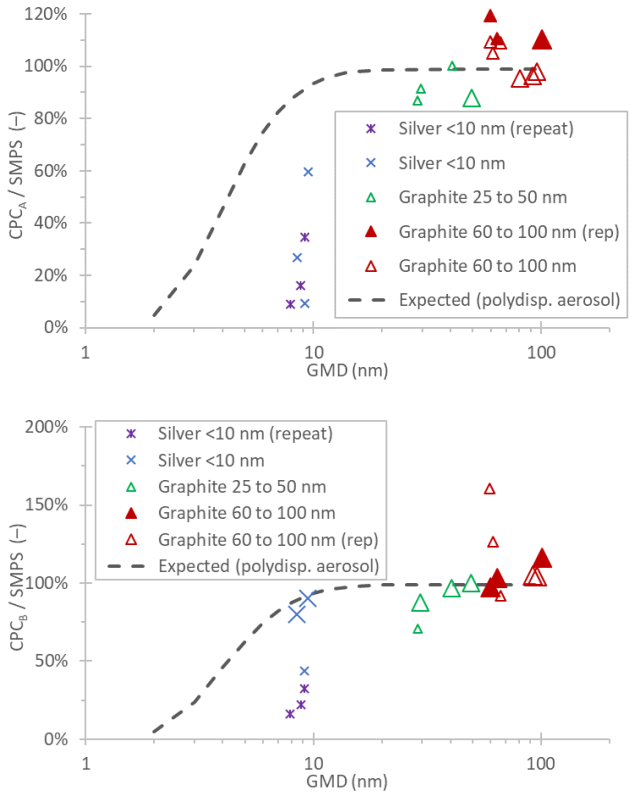

Fig. 8. Ratio of CPCs relative to SMPS for polydisperse particles in function of the geometric mean diameter (GMD). Dotted line is the expected curve for polydisperse aerosol based on the typical counting efficiency of the same model. Small symbols are concentrations in photometric mode, while larger symbols are in single counting mode: (a) CPC_A; (b) CPC_B

The previous studies can explain why there is a lower detection efficiency for smaller particle sizes, but they cannot explain why this difference varies with particle concentration (for the same size). Particle concentrations can also influence pulse-heights through vapor depletion as it was shown theoretically for the TSI 3022A [46] and for a TSI water CPC 3785 [47]. Experimentally it was found that pulse heights drop linearly with increasing concentration for all particle sizes [16]. However, the pulse height difference for particles of different initial size is a very weak function of aerosol concentration. A detailed theoretical study clearly demonstrated that at high particle number concentrations the super-saturation ratios decrease due to [48]: (i) depletion of the working fluid vapor due to the uptake by the droplets, and (ii) increase in the equilibrium vapor pressure due to warming of the flow from condensational heat release. Thus, with increasing particle number concentrations, the critical activation diameters increase and the final droplet sizes are smaller [48]. The later activation also results in smaller droplets due to less time in the condenser, as discussed previously. Concluding, the calibration should be model specific and in function of the particle concentration. Our results with the rest of the studies indicate that the calibration is valid only in the plateau region of the CPC, and attention is needed at small particle sizes.

Although less pronounced than for small sizes, why the calibration was not valid for big particles is not entirely clear. A plausible explanation is that the calibration was done at around 50 nm, for which the pulse height was not the maximum. Still some small differences of the final size can be seen for bigger particles, as they are activated earlier, although very small to fully explain this trend [41]. The linear pulse heights drop with increasing concentration probably is not taken into account correctly with the internal calibration functions. Another explanation could be the decrease of the droplet size with the temperature increase from the condenser to the optics. We are not aware of studies discussing this, and it's a topic that needs further investigation.

Finally, the influence of particle composition on pulse heights was also studied by other researchers [16]. Sulfuric acid and tungsten oxide particles had the same pulse height dependence with size below 10 nm [16, 43], while above 10 nm the dependency was very small in function of size. NaCl had differences at sizes < 10 nm, but they were attributed to the cubic shape of NaCl particles. For the same electrical mobility diameter, the length of the cube is 0.72 times the diameter of a sphere [16]. Thus, for the same electrical mobility size, the cube length is smaller and the activation more difficult. Based on these findings, the researchers concluded that the pulse height is not affected by the chemical composition, but weakly on the shape (surface area). Differences in the counting efficiencies in the cut-off curve have been reported by many researchers testing in the single counting mode [49–51]. These findings justify why there were no differences of the material in the plateau region (25 to 50 nm range) in the photometric mode for graphite, soot, and salt particles in our previous study [14].

Summarizing, the pulses depend on the size of particles and the particle number concentration. The chemical composition probably does not have any impact in the plateau region, but shape could have an effect at the steep part of the efficiency curve. However, at the sub-10 nm region, most particles are spherical so the shape impact should be negligible for most applications in practice. The key findings of this study is that the photometric mode needs detailed calibration in function of (i) the concentration and (ii) size, similar to what is done for the single counting mode for each instrument. For one of the tested CPCs the valid range (around 25 to 50 nm) was appropriate for PEMS

which measure from approximately 23 nm, but not for PTI instruments which are calibrated at 70 to 80 nm.

The key messages of this study are: (i) current calibrations in the photometric mode (if any) are not sufficient. Typically, no data are provided or in some cases a single concentration point. The material and the size is often not reported; (ii) more studies are necessary to confirm the findings of this study and whether the impact of concentration and size can be extrapolated to other designs. At the moment the use of the photometric mode for regulatory PEMS and PTI tests should be avoided; (iii) future calibration certificates should cover the concentration range of the photometric range and the size range of validity.

5. Conclusions

In this study we assessed two TSI 3752 CPCs in the photometric mode with silver and graphite particles in the size range of 10 nm to 100 nm. The two CPCs were within ±20% up to 10^6 #/cm^3 but had higher difference at higher concentrations. The differences were independent from the material indicating that one of them needed better calibration in the photometric mode. When a SMPS or a CPC downstream of a diluter (in order to keep it in single counting mode) were the reference instrument, it was found out that the silver 10 nm particles were almost linearly underestimated with increasing concentration. The underestimation was around –50% at 10^6 #/cm^3, reaching –90% at 10^7 #/cm^3. Large particles > 60 nm were overestimated around 50% at 3×10^6 #/cm^3 exceeding 100% at 10^7 #/cm^3. Only particles in the size range of 25 nm to 50 nm were accurately measured in the whole concentration range for one of the CPCs.

The behavior for small particles was attributed to the different position and time of particles activation in the condenser and consequently the different final size before optical detection. The resulting smaller final growth of smaller particles resulted in different scattered light and consequently particle number concentration. The particle concentration due to vapor depletion and condensational heat release reduced the super-saturations, and consequently resulted in larger activation diameters and smaller final droplet sizes. Consequently, smaller particles had an increasing deviation from the reference instrument in function of the concentration. The behavior for large particles needs further investigation, but it could be related to the internal calibration curve optimized for mid-sized particles. The important message is that the photometric mode should be avoided, and used only when its calibration remains unaffected in the size range of interest for the specific application.

Acknowledgements

The authors would like to acknowledge Dominique Lesueur for the support in the execution of the tests.

Disclaimer

The opinions expressed in this manuscript are those of the authors and should in no way be considered to represent an official opinion of the European Commission. Mention of trade names or commercial products does not constitute endorsement or recommendation by the authors or the European Commission.

Nomenclature

AIM aerosol instruments manager
CPC condensation particle counter
DEHS di-ethyl-hexyl-sebacate
DIL diluter
DMA differential mobility analyzer
EU European Union
GMD geometric mean diameter
GWG glowing wire generator
ISC in-service confirmity
NRMM non-road mobile machinery
PEMS portable emissions measurement system
PM particulate matter
PN particle number
PNC particle number counter
PTI periodic technical inspection
RDE real-driving emissions
SMPS scanning mobility particle sizer
USA United States of America

Bibliography

[1] Giechaskiel B, Mamakos A, Andersson J, Dilara P, Martini G, Schindler W et al. Measurement of automotive nonvolatile particle number emissions within the European legislative framework: a review. Aerosol Sci Tech. 2012;46:719-749. https://doi.org/10.1080/02786826.2012.661103

[2] Giechaskiel B, Melas A, Martini G, Dilara P. Overview of vehicle exhaust particle number regulations. Processes. 2021;9:2216. https://doi.org/10.3390/pr9122216

[3] Giechaskiel B, Lähde T, Suarez-Bertoa R, Clairotte M, Grigoratos T, Zardini A et al. Particle number measurements in the European legislation and future JRC activities. Combustion Engines. 2018;174(3):3-16. https://doi.org/10.19206/CE-2018-301

[4] Grigoratos T, Mamakos A, Arndt M, Lugovyy D, Anderson R, Hafenmayer C et al. Characterization of particle number setups for measuring brake particle emissions and comparison with exhaust setups. Atmosphere. 2023;14:103. https://doi.org/10.3390/atmos14010103

[5] Pajdowski P, Woodburn J, Bielaczyc P, Puchałka B. Development of RDE/ISC test methodology in light of Euro 6d/VI emissions limits. Combustion Engines. 2019;178(3):274-282. https://doi.org/10.19206/CE-2019-348

[6] Giechaskiel B, Bonnel P, Perujo A, Dilara P. Solid particle number (SPN) portable emissions measurement systems (PEMS) in the European legislation: a review. IJERPH 2019;16:4819. https://doi.org/10.3390/ijerph16234819

[7] Czerwiński J, Zimmerli Y, Hussy A, Engelmann D, Bonsack P, Remmele E et al. Testing and evaluating real driving emissions with PEMS. Combustion Engines. 2018;174(3):17-25. https://doi.org/10.19206/CE-2018-302

[8] Merkisz J, Pielecha J. Observations from PEMS testing of combustion engines of different applications. Combustion Engines. 2018;174(3):40-55. https://doi.org/10.19206/CE-2018-305

[9] McMurry PH. The history of condensation nucleus counters. Aerosol Sci Tech. 2000;33:297-322. https://doi.org/10.1080/02786820050121512
[10] Giechaskiel B, Maricq M, Ntziachristos L, Dardiotis C, Wang X, Axmann H et al. Review of motor vehicle particulate emissions sampling and measurement: From smoke and filter mass to particle number. J Aerosol Sci. 2014;67:48-86. https://doi.org/10.1016/j.jaerosci.2013.09.003
[11] Burtscher H, Lutz Th, Mayer A. A new periodic technical inspection for particle emissions of vehicles. Emiss Control Sci Technol. 2019;5:279-287. https://doi.org/10.1007/s40825-019-00128-z
[12] Melas A, Selleri T, Suarez-Bertoa R, Giechaskiel B. Evaluation of measurement procedures for Solid Particle Number (SPN) measurements during the Periodic Technical Inspection (PTI) of Vehicles. IJERPH 2022;19:7602. https://doi.org/10.3390/ijerph19137602
[13] Czerwiński J, Comte P. Testing emissions of passenger cars in laboratory and on-road (PEMS, RDE). Combustion Engines. 2016;166(3):17-23. https://doi.org/10.19206/CE-2016-326
[14] Giechaskiel B, Melas A. Comparison of particle sizers and counters with soot-like, salt, and silver particles. Atmosphere. 2022;13:1675. https://doi.org/10.3390/atmos13101675
[15] Ankilov A, Baklanov A, Colhoun M, Enderle K-H, Gras J, Yu J et al. Intercomparison of number concentration measurements by various aerosol particle counters. Atmos Res. 2002;62:177-207. https://doi.org/10.1016/S0169-8095(02)00010-8
[16] Saros MT, Weber RJ, Marti JJ, McMurry PH. Ultrafine aerosol measurement using a condensation nucleus counter with pulse height analysis. Aerosol Sci Tech. 1996;25:200-213. https://doi.org/10.1080/02786829608965391
[17] Tartakovsky L, Fleischman R. DPF retrofit program in Israel – effects of diesel particle filters on performance of in-use buses. Combustion Engines. 2017:176-178. https://doi.org/10.19206/CE-2017-330
[18] Olczyk M, Hejny B, Bielaczyc P. An overview of particle number emission from direct injection SI engine in scope of new legislation rules. Combustion Engines. 2015;163(4):67-78. https://doi.org/10.19206/CE-116858
[19] Czerwiński J, Comte P, Keller A, Mayer A. Investigations of nanoparticle emissions of two gasoline cars MPI & DI at stationary part load operation. Combustion Engines. 2014; 158(3):3-11. https://doi.org/10.19206/CE-116932
[20] Stabile L, Cauda E, Marini S, Buonanno G. Metrological assessment of a portable analyzer for monitoring the particle size distribution of ultrafine particles. Ann Occup Hyg. 2014;58:860-876. https://doi.org/10.1093/annhyg/meu025
[21] Jaroń A, Borucka A, Sobecki G. Assessment of the possibility of using nanomaterials as fuel additives in combustion engines. Combustion Engines. 2022;189(2):103-112. https://doi.org/10.19206/CE-143824
[22] Andres H, Lüönd F, Schlatter J, Auderset K, Jordan-Gerkens A, Nowak A et al. Measuring soot particles from automotive exhaust emissions. EPJ Web of Conferences 2014;77: 00020. https://doi.org/10.1051/epjconf/20147700020
[23] Hagen F, Hardock F, Koch S, Sebbar N, Bockhorn H, Loukou A et al. Why soot is not alike soot: A molecular/nanostructural approach to low temperature soot oxidation. Flow Turbulence Combust. 2021;106:295-329. https://doi.org/10.1007/s10494-020-00205-2
[24] Helsper C, Mölter W, Löffler F, Wadenpohl C, Kaufmann S, Wenninger G. Investigations of a new aerosol generator for the production of carbon aggregate particles. Atmos Environ A-Gen. 1993;27:1271-1275. https://doi.org/10.1016/0960-1686(93)90254-V
[25] Burtscher H, Schmidt-Ott A, Siegmann HC. Photoelectron yield of small silver and gold particles suspended in gas up to a photon energy of 10 eV. Z Physik B – Condensed Matter. 1984;56:197-199. https://doi.org/10.1007/BF01304172
[26] TSI Inc. Model 3752 Condensation Particle Counter Operation Manual, P/N 6011194, Revision D 2022.
[27] Hammer T, Irwin M, Swanson J, Berger V, Sonkamble U, Boies A et al. Characterising the silver particle generator; a pathway towards standardising silver aerosol generation. J Aerosol Sci. 2022;163:105978. https://doi.org/10.1016/j.jaerosci.2022.105978
[28] Liu PSK, Deshler T. Causes of concentration differences between a scanning mobility particle sizer and a condensation particle counter. Aerosol Sci Tech. 2003;37:916-923. https://doi.org/10.1080/02786820300931
[29] Tabrizi NS, Ullmann M, Vons VA, Lafont U, Schmidt-Ott A. Generation of nanoparticles by spark discharge. J Nanopart Res. 2009;11:315-332. https://doi.org/10.1007/s11051-008-9407-y
[30] Peineke C, Attoui MB, Schmidt-Ott A. Using a glowing wire generator for production of charged, uniformly sized nanoparticles at high concentrations. J Aerosol Sci. 2006; (37):1651-1661. https://doi.org/10.1016/j.jaerosci.2006.06.006
[31] Sinclair D, Hoopes GS. A continuous flow condensation nucleus counter. J Aerosol Sci. 1975;6:1-7. https://doi.org/10.1016/0021-8502(75)90036-1
[32] Agarwal JK, Sem GJ. Continuous flow, single-particle-counting condensation nucleus counter. J Aerosol Sci. 1980; (11):343-357. https://doi.org/10.1016/0021-8502(80)90042-7
[33] Sem GJ. Design and performance characteristics of three continuous-flow condensation particle counters: a summary. Atmos Res. 2002;62:267-294. https://doi.org/10.1016/S0169-8095(02)00014-5
[34] Asbach C, Schmitz A, Schmidt F, Monz C, Todea AM. Intercomparison of a personal CPC and different conventional CPCs. Aerosol Air Qual Res. 2017;17:1132-1141. https://doi.org/10.4209/aaqr.2016.10.0460
[35] Bau S, Toussaint A, Payet R, Witschger O. Performance study of various Condensation Particle Counters (CPCs): development of a methodology based on steady-state airborne DEHS particles and application to a series of handheld and stationary CPCs. J Phys: Conf Ser. 2017;838:012002. https://doi.org/10.1088/1742-6596/838/1/012002
[36] Gilham RJJ, Quincey PG. Measurement and mitigation of response discontinuities of a widely used condensation particle counter. J Aerosol Sci. 2009;40:633-637. https://doi.org/10.1016/j.jaerosci.2009.03.004
[37] Biswas S, Fine PM, Geller MD, Hering SV, Sioutas C. Performance evaluation of a recently developed water-based condensation particle counter. Aerosol Sci Tech. 2005;39: 419-427. https://doi.org/10.1080/027868290953173
[38] Stolzenburg MR, McMurry PH. An ultrafine aerosol condensation nucleus counter. Aerosol Sci Tech. 1991;14:48-65. https://doi.org/10.1080/02786829108959470
[39] Reinisch T, Radl S, Bergmann A, Schriefl M, Kraft M. Effect of model details on the predicted saturation profiles in condensation particle counters. Adv Powder Technol. 2019; (30):1625-1633. https://doi.org/10.1016/j.apt.2019.05.011
[40] Giechaskiel B, Wang X, Gilliland D, Drossinos Y. The effect of particle chemical composition on the activation probability in n-butanol condensation particle counters. J Aerosol Sci. 2011;42:20-37. https://doi.org/10.1016/j.jaerosci.2010.10.006
[41] Mamakos A, Giechaskiel B, Drossinos Y. Experimental and theoretical investigations of the effect of the calibration aerosol material on the counting efficiencies of TSI 3790 con-

densation particle counters. Aerosol Sci Tech. 2013;47:11-21. https://doi.org/10.1080/02786826.2012.716174
[42] Su YF, Cheng YS, Newton GJ, Yeh HC. Counting efficiency of the TSI model 3020 condensation nucleus counter. Aerosol Sci Tech. 1990;12:1050-1054. https://doi.org/10.1080/02786829008959414
[43] Weber RJ, Stolzenburg MR, Pandis SN, McMurry PH. Inversion of ultrafine condensation nucleus counter pulse height distributions to obtain nanoparticle (~3–10 nm) size distributions. J Aerosol Sci. 1998;29:601-615. https://doi.org/10.1016/S0021-8502(97)10026-X
[44] Ham S, Lee N, Eom I, Lee B, Tsai P-J, Lee K et al. Comparison of real time nanoparticle monitoring instruments in the workplaces. Safety and Health at Work. 2016;7:381-388. https://doi.org/10.1016/j.shaw.2016.08.001
[45] Watson JG, Chow JC, Sodeman DA, Lowenthal DH, Chang M-CO, Park K et al. Comparison of four scanning mobility particle sizers at the Fresno Supersite. Particuology. 2011; (9):204-209. https://doi.org/10.1016/j.partic.2011.03.002
[46] Wu C-Y, Biswas P. Particle growth by condensation in a system with limited vapor. Aerosol Sci Tech. 1998;28:1-20. https://doi.org/10.1080/02786829808965508
[47] Stratmann F, Herrmann E, Petäjä T, Kulmala M. Modelling Ag-particle activation and growth in a TSI WCPC model 3785. Atmos Meas Tech. 2010;3:273-281. https://doi.org/10.5194/amt-3-273-2010
[48] Lewis GS, Hering SV. Minimizing concentration effects in water-based, laminar-flow condensation particle counters. Aerosol Sci Tech. 2013;47:645-654. https://doi.org/10.1080/02786826.2013.779629
[49] Chen L, Zhang X, Zhang C, Raza M, Li X. Experimental investigation of a condensation particle counter challenged by particles with varying wettability to working liquid. Aerosol Air Qual Res. 2017;17:2743-2750. https://doi.org/10.4209/aaqr.2017.06.0201
[50] Giechaskiel B, Wang X, Horn H-G, Spielvogel J, Gerhart C, Southgate J et al. Calibration of condensation particle counters for legislated vehicle number emission measurements. Aerosol Sci Tech. 2009;43:1164-1173. https://doi.org/10.1080/02786820903242029
[51] Wang X, Caldow R, Sem GJ, Hama N, Sakurai H. Evaluation of a condensation particle counter for vehicle emission measurement: Experimental procedure and effects of calibration aerosol material. J Aerosol Sci. 2010;41:306-318. https://doi.org/10.1016/j.jaerosci.2010.01.001

Barouch Giechaskiel, PhD – European Commission, Joint Research Centre (JRC), Ispra 21027, Italy.
e-mail: *Barouch.Giechaskiel@ec.europa.eu*

Anastasios Melas, PhD – European Commission, Joint Research Centre (JRC), Ispra 21027, Italy.
e-mail: *Anastasios.Melas @ec.europa.eu*

Athanasios Mamakos, PhD – Corning GmbH, Wiesbaden 65189, Germany.
e-mail: *MamakosA@corning.com*